SCIENCE CHINA
Information Sciences

• RESEARCH PAPER •

October 2023, Vol. 66 200410:1–200410:6
https://doi.org/10.1007/s11432-023-3759-x

Special Topic: Recent Progress of Fundamental Research on Post-Moore Novel Devices

Ferroelectric-like behaviors of metal-insulator-metal with amorphous dielectrics

Huan LIU[1,2], Jiajia CHEN[1], Chengji JIN[1], Xiao YU[1*], Yan LIU[2*] & Genquan HAN[1,2]

[1] *Research Center for Intelligent Chips, Zhejiang Lab, Hangzhou 311121, China;*
[2] *School of Microelectronics, Xidian University, Xi'an 710071, China*

Received 31 January 2023/Revised 15 March 2023/Accepted 5 May 2023/Published online 31 August 2023

Abstract In this paper, unique ferroelectric-like characteristics in amorphous (a-) ZrO_2-based devices enabled by mobile ions are systematically investigated at room temperature and cryogenic. The physical origin of the ferroelectric-like behaviors of the metal/a-ZrO_2/metal capacitor is confirmed to be the migration of ions exhibiting strong frequency dependency due to the limited velocity of the mobile ions, which is proven by the comparison between experimental results and theoretical analysis. The ferroelectric-type hysteresis will be reduced sharply with the decrease of the temperature, which is essentially different from the reported doped-HfO_2 FeFET. This further confirms that the origin of the ferroelectric-like characteristics is the migration and redistribution of the mobile ions.

Keywords ferroelectric-like, mobile ion, amorphous dielectric, ZrO_2, temperature

Citation Liu H, Chen J J, Jin C J, et al. Ferroelectric-like behaviors of metal-insulator-metal with amorphous dielectrics. Sci China Inf Sci, 2023, 66(10): 200410, https://doi.org/10.1007/s11432-023-3759-x

1 Introduction

Great research efforts have been devoted to exploring ferroelectric materials for promising potential applications in emerging non-volatile memory (NVMs) [1–3], negative capacitance field-effect transistors [4], in-memory computing [5, 6], and artificial synapse [7]. Recent observations of ferroelectricity in polycrystalline HfO_2-based materials have attracted great interest due to their better thickness scalability and CMOS process compatibility [8, 9]. Ferroelectric behavior in doped HfO_2 thin films was associated with its non-centrosymmetric orthorhombic phase. However, the wake-up effect remains a major problem for HfO_2-based ferroelectric thin films. Additionally, limited endurance due to the ferroelectric phase change and the charge trapping during the polarization switching and the nature of polycrystalline structure leading to undesired leakage current are still an obstacle in the commercialization of hafnia-based ferroelectric materials [10, 11].

Besides the polycrystalline ferroelectric HfO_2, the ferroelectric-like behavior also has been observed in devices with amorphous (a-) dielectrics (ZrO_2, Al_2O_3, HfO_2, etc.), which shows advantages in the thermal budget, endurance, operation voltage, and scaling limits, and has been demonstrated for non-volatile memory and neuromorphic application [12–16]. Although the ferroelectric-like phenomenon of the amorphous film was considered oxygen-vacancies related [15, 17], the physical origin for the ferroelectric like behaviors and essential differences from doped-HfO_2 FeFETs have not been revealed yet.

In this work, we systematically investigate the unique frequency (f) and temperature (T) dependency of characteristics of the FE-like metal-insulator-metal capacitors with amorphous dielectric. The calculation results utilizing the ion drift-diffusion model agree well with the experimental data indicating that the ferroelectric-like behaviors originate from the migration of the mobile ions.

* Corresponding author (email: yuxiao@zhejianglab.com, xdliuyan@xidian.edu.cn)

© Science China Press 2023

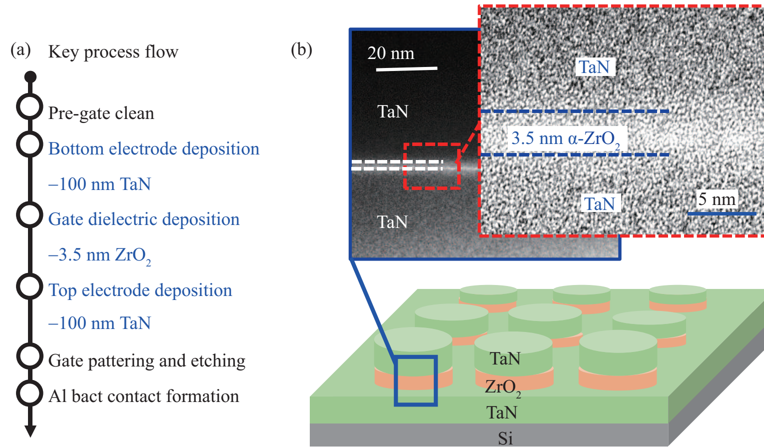

Figure 1 (Color online) (a) Key process steps for fabricating a-ZrO_2-based MIM; (b) schematic illustration and corresponding HRTEM images of the fabricated TaN/a-ZrO_2/TaN MIM capacitors.

2 Device fabrication

Amorphous-ZrO_2 MIM capacitors have been fabricated. Key process steps are shown in Figure 1(a). TaN as bottom metal layers was deposited on the P^+-Si substrate by reactive sputtering. The a-ZrO_2 film with thicknesses of 3.5 nm was deposited on the bottom metal layer by atomic layer deposition (ALD) at 250°C. The ALD deposition precursors of Zr and O are $Zr[N(CH_3)_2]_4$ and H_2O, respectively. To increase the concentration of oxygen vacancies, we intentionally choose oxygen-deficient conditions for ZrO_2 deposition [17]. After the top metal layer deposition, MIM capacitors were fabricated by lithography patterning and dry etching. Here, any thermal treatments such as post-metallization annealing during the gate stack formation were prevented. The polarization switching properties of the devices were characterized by an aixACCT TF Analyzer 2000. The electrical characteristics were measured using the Tektronix 4200A-SCS and vacuum chamber with a liquid helium environment, which can reduce the measurement temperature to 3.5 K.

Figure 1(b) shows the schematic illustration of the TaN/ZrO_2/TaN MIM capacitors and high-resolution transmission electron microscope (HRTEM) images of the fabricated MIM. The amorphous ZrO_2 layers with a thickness of 3.5 nm have been confirmed from the images, which is consistent with the fabrication process in that crystalline annealing was prevented.

3 Results and discussion

Charge-voltage (Q-V) curves of the ZrO_2 MIM structures are measured by applying a triangular waveform at 1 kHz with various sweeping voltages, as shown in Figure 2(a). The obvious ferroelectric-like Q-V curves can be achieved, but also in thicker a-ZrO_2 dielectric. Similar to the remnant polarization (P_r) in ferroelectric film, we define Q_r as the values of charge @$V = 0$ of Q-V curves to evaluate the intensity of ferroelectric-like behaviors. Q_r increases with increasing voltage amplitude. To eliminate the impact of leakage current, positive-up, negative-down (PUND) pulsed measurements were used, as shown in Figure 2(b). The current responses in two continuous pulses are different, which results in finite Q_r and thus hysteresis. The results indicate that the ferroelectric-type behaviors are not induced by leakage current. On the other hand, this kind of behavior is quite different from ferroelectric which exhibits polarization switching current peak [18].

To discriminate the characteristics of the ferroelectric-like behaviors, the frequency dependency of Q-V characteristics has been investigated. Figure 3(a) shows the Q-V curves of the TaN/a-ZrO_2/TaN capacitor measured with triangular waveforms at a frequency varying from 1 to 100 kHz. It is observed that the Q-V loops of the device strongly depend on the measurement frequency, and Q_r will increase at a lower frequency. This kind of behavior is quite different from poly-crystalline ferroelectric $HfZrO_x$ (HZO) for which polarization switching has a much smaller dependence on frequency in a range of 1 kHz to 1 MHz, indicating the mechanism for Q-V hysteresis of the a-ZrO_2 film is different from polarization switching of the ferroelectric thin films.

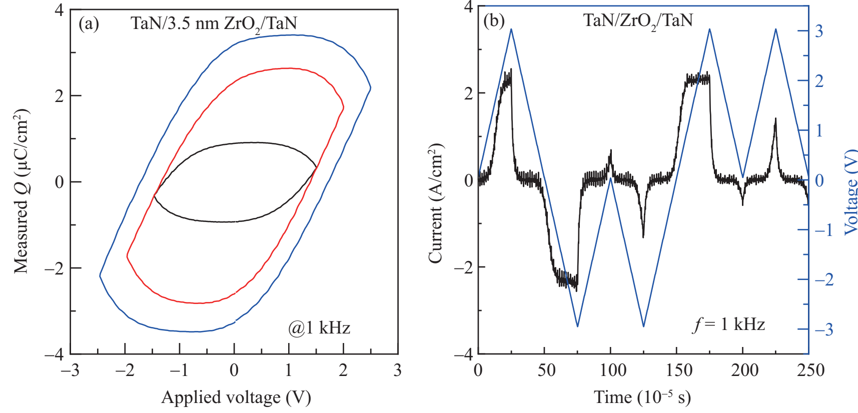

Figure 2 (Color online) (a) Q-V curves of the MIM capacitors at 1 kHz. Ferroelectric-like behaviors can be observed. (b) PUND measurement of MIM capacitor at 1 kHz.

One possibility for such a strong frequency dependence can be the ion drift mechanism. To get a deep insight into the physical origin of a ferroelectric-like phenomenon, we performed numerical simulations of the polarization switching based on the ion drift-diffusion model, considering mobile oxygen vacancies (V_o^{2+}) and oxygen ions (O^{2-}). The equation of the ion drift-diffusion model can be described as

$$\frac{\partial n_{v/o}}{\partial t} = D_{v/o}\frac{\partial^2 n_{v/o}}{\partial x^2} + \mu_{v/o}\frac{\partial}{\partial x}(E_x \cdot n_{v/o}), \tag{1}$$

where n_o, n_v, D_o, D_v, μ_o, and μ_v represent the mobile ion concentration, the diffusion coefficient, and the mobility of the mobile O^{2-} and V_o^{2+} in the dielectric, respectively. The potential φ can be derived from the 1D Poisson's equation as follows:

$$\frac{\partial^2 \varphi}{\partial x^2} = -\frac{2q(n_v - n_o)}{\varepsilon_r \varepsilon_0}, \tag{2}$$

where ε_r and ε_0 are relative permittivities and vacuum permittivity, respectively, and q is the charge of an electron.

According to the previous study, it is reasonable to assume that the charged ions can drift in dielectric and stay at the interface under an electric field [17]. The values of D_o, D_v, μ_o, and μ_v calibrated by the experimental data in the previous work [19] are set to 5.49×10^{-14} cm^2/s, 1.10×10^{-14} cm^2/s, 4.12×10^{-9} cm^2/V $\cdot$ s, and 8.24×10^{-13} cm^2/V $\cdot$ s, respectively. And a reasonable assumption has been proposed that the drift velocity of O^{2-} is much larger than those of V_o^{2+} according to the previous study [20]. By solving the ion drift-diffusion equation (1) coupling with Poisson's equation (2), the distribution of mobile ions and the charge at the electrode as a function of time or applied voltage can be obtained. The simulated Q-V hysteresis curves with various frequencies are plotted in Figure 3(b). The simulation has provided similar Q-V curves and their frequency dependency to the experimental results. The measurement results can be qualitatively reproduced, indicating the physical origin of the ferroelectric-like behaviors should be mobile ions in amorphous film. For a better understanding of the hysteresis curve induced by mobile ions, we further investigate the distributions of mobile ions along dielectric thickness at different operation points as indicated by A–F in Figure 3(c). Noting that the diffusion coefficient and the mobility of positive and negative ions should be quite different, the movement of V_o^{2+} can be ignored compared with the movement of O^{2-}. The negative slope shown in the upper right corner from state C to D of the Q-V curve is because there is still an external electric field strong enough to cause the drift of oxygen to be higher than the diffusion of oxygen, increasing of the accumulated O^{2-} charge near the metal/dielectric interface. Figure 3(d) compares the extracted Q_r vs. frequency performance, for the measured a-ZrO_2 MIM capacitor and the reported HZO and La_2O_3 devices [21, 22]. Noted that P_r in HZO is less frequency-sensitive than the amorphous ferroelectric-like dielectrics, P_r slightly reduced at high frequency is due to the voltage drop on the resistance in series with HZO film. Compared with the previously reported mobile-ionic dielectrics such as La_2O_3, or Ta_2O_5 [22, 23], the switching speed of a-ZrO_2 MIM capacitor is faster by over 3 orders, which can be attributed to the smaller thickness of a-ZrO_2, and the higher mobility of the oxygen vacancies. Such

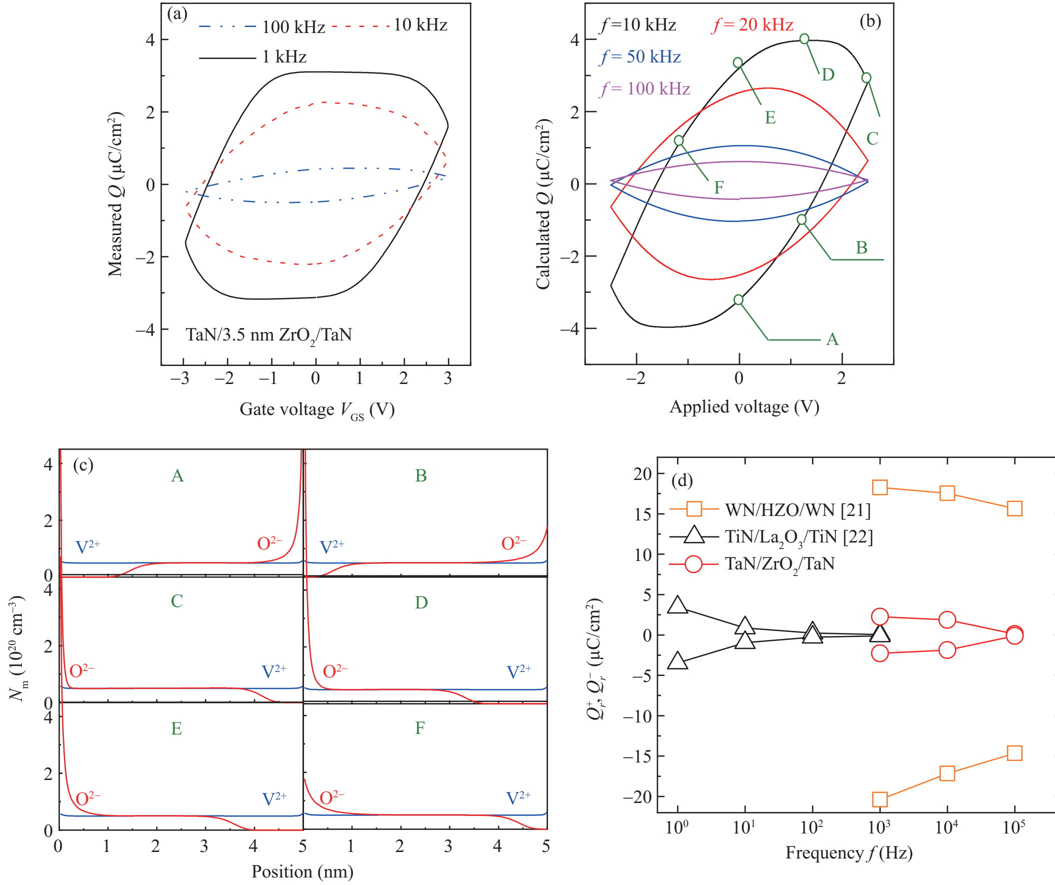

Figure 3 (Color online) (a) Measured and (b) simulated Q-V hysteresis loops of TaN/a-ZrO_2/TaN capacitor at different f. (c) Charge distribution in each point in (b). (d) Q_r vs. f for the measured a-ZrO_2 capacitor and the reported HZO and La_2O_3 devices.

switching speed makes it favorable for memory applications. On the other hand, a variety of these devices with time-dependent characteristics will have the potential for artificial intelligence (AI) applications [16].

To further evaluate the FE-like behaviors of the proposed a-ZrO_2-based MIM induced by mobile ions, the temperature dependence of Q-V curves in a wide temperature ranging from 200 down to 50 K has been measured, as shown in Figure 4(a). As the temperature decreases, the Q_r will shrink, which is consistent with the nature of mobile ions since the drift-diffusion of mobile ions is strongly related to the temperature. The charge density dependence on the temperature is also incorporated inside the model, the simulated Q-V hysteresis curves with various temperatures are plotted in Figure 4(b). Here, we have made a reasonable assumption that the value of activation energy of oxygen ion in amorphous ZrO_2 film is 0.22 eV according to the previous work [19]. The mobility is related to the activation energy and temperature. The obtained Q_r agrees well with the measured a-ZrO_2-based MIM. The mobility of oxygen vacancies can be significantly depressed at reduced temperatures, resulting in a decrease in the vacancy diffusion coefficient. Additionally, the increasing activation energy related to the temperature may also reduce the diffusion coefficient. However, the HZO MFM shown in Figure 4(c) exhibits a larger coercive field (E_c) and lower Q_r as decreased temperature, the underlying mechanism was attributed to the fact that its E_c getting closer to the intrinsic value at the cryogenic temperature, resulting in unsaturated polarization hysteresis loops [24]. It should be noted that although the mobile ion behavior degrades at low temperatures, ferroelectric-like characteristics will be improved by the larger applied voltage and slower pulse.

The endurance and retention characteristics of a-ZrO_2 MIM capacitors are measured, as shown in Figures 5(a) and (b), respectively. Over 10^5 cycles of endurance have been achieved with a pulse scheme of 1 kHz without wake-up and fatigue effects, which are long-standing issues for ferroelectric devices. The retention over 10^4 s with negligible degradation is experimentally demonstrated, which shows potential for practical NVM. Such endurance and retention properties are consistent with the reported data based

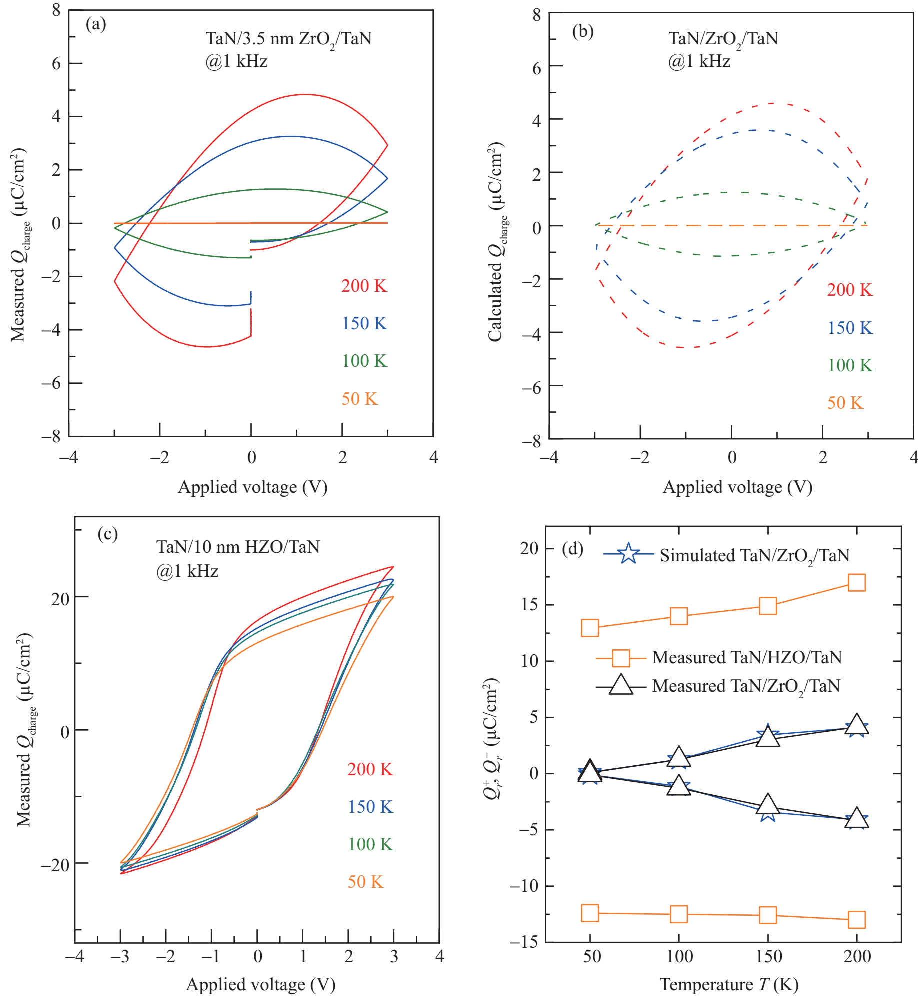

Figure 4 (Color online) Measured (a) and simulated (b) Q-V hysteresis curves of a-ZrO_2-MIM capacitor for various temperatures from 200 to 50 K; (c) measured P-V curves of HZO devices with various temperatures; (d) Q_r vs. T for the a-ZrO_2 capacitor and the HZO devices.

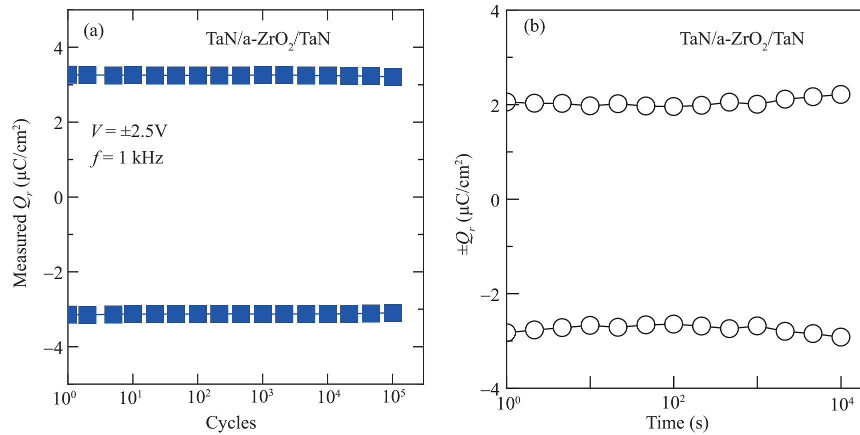

Figure 5 (Color online) (a) Endurance characteristics at 1 kHz and (d) retention characteristics for a-ZrO_2 MIM capacitors.

on the amorphous film. It is important to emphasize that the wake-up effect in doped-HfO_2 FeFETs can be attributed to the diffusion of the oxygen vacancies under the electric field [11]. Additionally, high oxygen vacancy content in HZO films will decrease P_r and degrade the endurance [25], which should be avoided. On the other hand, the oxygen vacancy in non-volatile FET related to ferroelectric-like behavior

exhibits a small P_r and no wake-up effect, which is beneficial to endurance characteristics.

4 Conclusion

In summary, the frequency and temperature dependency of the FE-like characteristics of MIM capacitors with amorphous ZrO_2 has been evaluated. The theoretical calculation based on the ion drift-diffusion model shows consistency with the experimental data. These results indicate that mobile ions dominate the ferroelectric-like characteristics, which exhibit unique characteristics from ferroelectric with decent endurance without wake-up and fatigue effect, providing a potential technique for NVM and other novel applications.

Acknowledgements This work was supported by National Key Research and Development Project (Grant No. 2022ZD0119002), National Natural Science Foundation of China (Grant Nos. 62204226, 62025402, 62090033, 91964202, 62204229, 62204228), Major Scientific Research Project of Zhejiang Lab (Grant No. 2021MD0AC01), and Zhejiang Province Key R&D Programs (Grant Nos. 2022C01232, 2021C05004).

References

1 Ryu S, Han J, Moon D, et al. One-transistor nonvolatile SRAM (ONSRAM) on silicon nanowire SONOS. In: Proceedings of IEEE International Electron Devices Meeting (IEDM), 2009. 1–4
2 Park K H, Park C M, Kong S H, et al. Novel double-gate 1T-DRAM cell using nonvolatile memory functionality for high-performance and highly scalable embedded DRAMs. IEEE Trans Electron Devices, 2010, 57: 614–619
3 Li X, Ma K, George S, et al. Design of nonvolatile SRAM with ferroelectric FETs for energy-efficient backup and restore. IEEE Trans Electron Devices, 2017, 64: 3037–3040
4 Zhou J, Han G, Li Q, et al. Ferroelectric $HfZrO_x$ Ge and GeSn PMOSFETs with Sub-60 mV/decade subthreshold swing, negligible hysteresis, and improved I_{ds}. In: Proceedings of IEEE International Electron Devices Meeting (IEDM), 2016. 1–4
5 Yin G, Cai Y, Wu J, et al. Enabling lower-power charge-domain nonvolatile in-memory computing with ferroelectric FETs. IEEE Trans Circuits Syst II, 2021, 68: 2262–2266
6 Thirumala S, Jain S, Raghunathan A, et al. Non-volatile memory utilizing reconfigurable ferroelectric transistors to enable differential read and energy efficient in-memory computation. In: Proceedings of IEEE/ACM International Symposium on Low Power Electronics and Design, 2019. 1–6
7 Jerry M, Chen P, Zhang J, et al. Ferroelectric FET analog synapse for acceleration of deep neural network training. In: Proceedings of IEEE International Electron Devices Meeting (IEDM), 2017. 1–4
8 Müller J, Böscke T S, Bräuhaus D, et al. Ferroelectric $Zr_{0.5}Hf_{0.5}O_2$ thin films for nonvolatile memory applications. Appl Phys Lett, 2011, 99: 112901
9 Müller J, Böscke S T, Müller S, et al. Ferroelectric hafnium oxide: a CMOS-compatible and highly scalable approach to future ferroelectric memories. In: Proceedings of IEEE International Electron Devices Meeting (IEDM), 2013. 1–4
10 Zheng Y, Zhong C, Zheng Y, et al. In-situ atomic visualization of structural transformation in $Hf_{0.5}Zr_{0.5}O_2$ ferroelectric thin film: from nonpolar tetragonal phase to polar orthorhombic phase. In: Proceedings of Symposium on VLSI Technology (VLSIT), 2021. 1–2
11 Starschich S, Menzel S, Böttger U. Evidence for oxygen vacancies movement during wake-up in ferroelectric hafnium oxide. Appl Phys Lett, 2016, 108: 32903
12 Liu H, Li J, Wang G, et al. Analog synapses based on nonvolatile FETs with amorphous ZrO_2 dielectric for spiking neural network applications. IEEE Trans Electron Devices, 2022, 69: 1028–1033
13 Peng Y, Xiao W, Han G, et al. Memory behavior of an Al_2O_3 gate dielectric non-volatile field-effect transistor. IEEE Electron Device Lett, 2020, 41: 1340–1343
14 Peng Y, Xiao W, Liu F, et al. Non-volatile field-effect transistors enabled by oxygen vacancy-related dipoles for memory and synapse applications. IEEE Trans Electron Devices, 2020, 67: 3632–3636
15 Liu H, Peng Y, Han G, et al. ZrO_2 ferroelectric field-effect transistors enabled by the switchable oxygen vacancy dipoles. Nanoscale Res Lett, 2020, 15: 120
16 Li Y, Fuller E J, Asapu S, et al. Low-voltage, CMOS-free synaptic memory based on Li_XTiO_2 redox transistors. ACS Appl Mater Interfaces, 2019, 11: 38982–38992
17 Feng Z, Peng Y, Shen Y, et al. Ferroelectric-like behavior in TaN/High-k/Si system based on amorphous oxide. Adv Electron Mater, 2021, 7: 2100414
18 Wu C, Ye H, Shaju N, et al. $Hf_{0.5}Zr_{0.5}O_2$-based ferroelectric gate HEMTs with large threshold voltage tuning range. IEEE Electron Device Lett, 2020, 41: 337–340
19 Chen J, Liu H, Jin C, et al. A physics-based model for mobile-ionic field-effect transistors with steep subthreshold swing. IEEE J Electron Devices Soc, 2022, 10: 706–711
20 Mo F, Tagawa Y, Saraya T, et al. Scalability study on fcrroclcctric-HfO_2 tunnel junction memory based on non-equilibrium green function method with selfconsistent potential. In: Proceedings of IEEE International Electron Devices Meeting (IEDM), 2018. 1–4
21 Lyu X, Si M, Sun X, et al. Ferroelectric and anti-ferroelectric hafnium zirconium oxide: scaling limit, switching speed and record high polarization density. In: Proceedings of Symposium on VLSI Technology, 2019. 44–45
22 Endo K, Kato K, Takenaka M, et al. Electrical characteristic of atomic layer deposition La_2O_3/Si MOSFETs with ferroelectric-type hysteresis. Jpn J Appl Phys, 2019, 58: SBBA05
23 Kumar A, Pillai P B, Song X, et al. Negative capacitance beyond ferroelectric switches. ACS Appl Mater Interfaces, 2018, 10: 19812–19819
24 Wang Z, Ying H, Chern W, et al. Cryogenic characterization of a ferroelectric field-effect-transistor. Appl Phys Lett, 2020, 116: 042902
25 Mittmann T, Materano M, Chang S, et al. Impact of oxygen vacancy content in ferroelectric HZO films on the device performance. In: Proceedings of IEEE International Electron Devices Meeting (IEDM), 2020. 1–4